ACS APPLIED POLYMER MATERIALS

pubs.acs.org/acsapm Article

Conducting Polymer-Based Electrochemical Aptasensor for the Detection of Adenosine

Damilola O. Runsewe, Grace Haya, Tania Betancourt,* and Jennifer A. Irvin*

Cite This: *ACS Appl. Polym. Mater.* 2021, 3, 6674–6683 Read Online

ACCESS | Metrics & More | Article Recommendations | Supporting Information

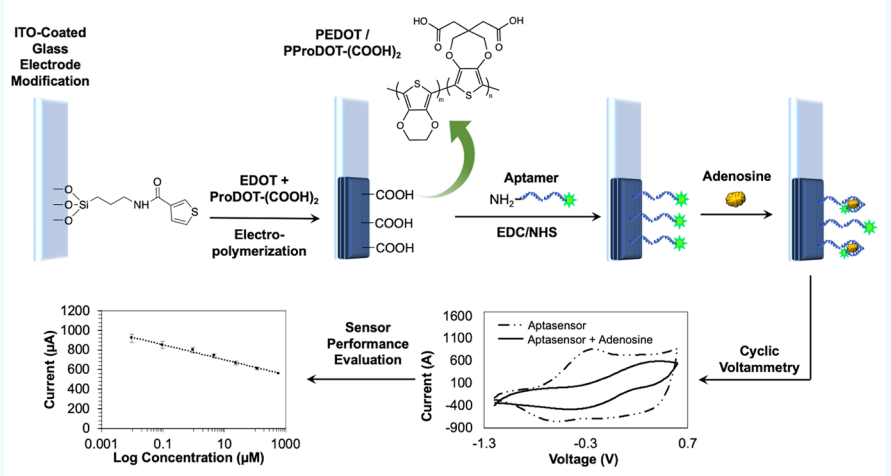

ABSTRACT: Emerging research in the area of conducting polymer-based electrochemical biosensors has revealed the need for the development of techniques that can enable easy functionalization with biorecognition molecules and enhance biosensor stability. In this work, an electrochemical biosensor for the detection of the small molecule adenosine was developed utilizing a conducting copolymer as a transducing agent. First, a method was developed to modify the surface of indium tin oxide-coated glass slides to enable robust copolymer deposition. A 3,4-ethylenedioxythiophene (EDOT) and 2*H*-thieno[3,4-*b*][1,4]dioxepin-3,3(4*H*)-diacetic acid (ProDOT−$(COOH)_2$) copolymer was then electrochemically grown on the surface of the modified slides. This copolymer was used to covalently attach an aptamer specific to adenosine to the biosensing platform to provide the system with target selectivity. The electroactivity of the conducting polymer before and after aptamer attachment in aqueous electrolyte solutions was studied. The attachment of the aptamers to the conducting polymer was confirmed using fluorescence microscopy and cyclic voltammetry. The fabricated aptamer-based sensors were then used for the electrochemical detection of adenosine, and the performance of the sensor was investigated. The adenosine aptasensor had a limit of detection of 2.33 nM and a linear range from 9.6 nM to 600 μM. The adenosine aptasensor showed good selectivity against competing interfering agents and specificity relative to scrambled oligonucleotide stands. In addition, the sensor showed good stability for up to 6 days when stored in 0.1 M phosphate-buffered saline or argon.

KEYWORDS: *conducting polymer, aptamer, biosensor, electrochemical detection, adenosine, cyclic voltammetry, PEDOT, ProDOT*

1. INTRODUCTION

Adenosine is a well-studied target that has been widely used as a model analyte in the development of aptamer-based biosensors.[1−4] Adenosine is an endogenous nucleoside modulator that is released from almost all cells and participates in biological processes including extension of blood vessels, antiarrhythmia, increase of blood flow, and improvement of oxygen supply to cardiac muscle.[5,6] In addition, it is an essential intermediate in the synthesis of adenine, adenylic acid, vidarabine, and adenosine triphosphate (ATP).[7,8] ATP is the main energy carrying component of cells. Abnormal ATP levels are associated with Alzheimer's and Parkinson's disesases.[9] ATP is typically released from dying cells; this constitutes one of the major independent hallmarks of immunogenic cell death from cancer treatment (such as chemotherapy and photothermal therapy).[10]

Received: October 8, 2021
Accepted: November 15, 2021
Published: November 24, 2021

https://doi.org/10.1021/acsapm.1c01348
ACS Appl. Polym. Mater. 2021, 3, 6674−6683

Aptamers are single-stranded nucleic acids, or peptides, that interact with molecular targets through noncovalent interactions with high affinity and specificity. Aptamers are selected from random oligonucleotide pools by the method known as the systematic evolution of ligands using exponential enrichment (SELEX), which was first reported by Gold[11] and Ellington and Szostak.[12] The characteristic ease of preparation of aptamer sequences via solid-phase synthesis, superior stability to denaturation at elevated temperatures, and high selectivity for a wider range of targets have made aptamers favorable over antibodies for the development of a wide range of sensors.[13−17]

Electrochemical affinity biosensors utilize biorecognition molecules to interact specifically with target analytes and combine the recognition event with an electrochemical transduction for analytical detection.[13−15,18−22] Electrochemical aptamer-based sensors (aptasensors) have been used for detecting various targets due to their high specificity, low instrumentation use, and lower production cost.[23] Electrochemical aptasensors that detect adenosine or ATP have utilized detection methods including differential pulse voltammetry,[24−26] cyclic voltammetry,[27,28] square wave voltammetry,[29,30] alternating current voltammetry,[31] and electrochemical impedance spectroscopy.[32] Cyclic voltammetry is a particularly promising method for rapid, inexpensive electrochemical detection; a $30 cyclic voltammetry-based biosensor controlled by a smartphone has already been demonstrated for point-of-care medical diagnostic testing.[33]

Various immobilization matrices such as inherently conducting polymers (CPs), carbonaceous materials (graphene, graphene oxide, and carbon nanotubes), bimetallic nanoparticles, metal oxides, and their combinations have been explored for their biosensing capabilities.[34−38] CPs consist of fully conjugated backbones that can be readily oxidized or reduced to introduce dopant ions and become conductive. In addition to conductivity, CPs exhibit changes in reactivity, color, and volume, leading to a wide range of applications including as sensors.[22,39−44] CPs can be used as electrochemical sensors if their characteristic electrochemical behavior changes reproducibly in the presence of an analyte.[22] Poly(3,4-ethylenedioxythiophene) (PEDOT) has been widely explored as a CP-based immobilization matrix due to its high conductivity, good electrochemical stability, and biocompatibility with other molecules.[45−49] Likewise, poly(3,4-propylenedioxythiophene) (PProDOT) and its derivatives have been explored as electrochemical biosensing platforms.[50,51] Both 3,4-ethylenedioxythiophene (EDOT) and 3,4-propylenedioxythiophene (ProDOT) can be functionalized on their ether side rings with functional groups that can be used to connect the CPs to biorecognition molecules. However, substituted EDOTs are typically unsymmetrical, while substituted ProDOTs are symmetrical and possibly easier to purify. Also, symmetrical polymers do not have regioirregularity concerns, so they are oftentimes more conductive.[52]

The synthesis of the ProDOT derivative 2*H*-thieno[3,4-*b*][1,4]dioxepin-3,3(4*H*)-diacetic acid (ProDOT−$(COOH)_2$) was reported by Beaujuge et al.[53] The group esterified the monomer prior to polymerization and then hydrolyzed the ester groups to form a water-soluble polymer salt that could be used in spray-coating applications. An asymmetric monocarboxylic acid-functionalized PProDOT derivative was also previously reported by Mantione et al.[54]

In this work, a CP-based electrochemical biosensor for the detection of adenosine and ATP was developed utilizing a copolymer of EDOT and ProDOT−$(COOH)_2$. This is the first time PProDOT−$(COOH)_2$ has been reported for use in biosensing applications. ProDOT−$(COOH)_2$ was selected to enable covalent immobilization of the adenosine aptamer, and EDOT was added to decrease the aqueous solubility. To enable the preparation of a robust, stable biosensor, the indium tin oxide (ITO) surface of the electrode was chemically modified with (3-aminopropyl)triethoxysilane (APTES) and 3-thiophenecarboxylic acid (3-Th-COOH) prior to electrochemical copolymerization of EDOT and ProDOT−$(COOH)_2$ to ensure covalent attachment of the polymer to the substrate. Adenosine was detected with the biosensor by cyclic voltammetry (CV). The electrochemical performance, selectivity, and stability after storage and use of the biosensor were investigated. The results were promising and could provide the opportunity for a reproducible electrochemical platform for detecting various analytes.

2. EXPERIMENTAL SECTION

2.1. Reagents and Materials. Tetrabutylammonium perchlorate (TBAP) was purchased from TCI Chemicals (Portland, OR, USA) and recrystallized from hot ethyl acetate. ITO-coated glass slides (CG-50IN-CUV: 8−12 ohms per square, 7 × 50 × 0.7 mm) were purchased from Delta Technologies (Loveland, CO, USA). APTES (98%) and 1-ethyl-3-(3-(dimethylamino)propyl)-carbodiimide (EDC) were purchased from Alfa Aesar (Haverhill, MA, USA). *N*-Hydroxysuccinimide (NHS) and ethanol were purchased from Thermo Fisher Scientific (Waltham, MA, USA). Acetonitrile was purchased from Acros Organics (New Jersey, USA). ProDOT−$(COOH)_2$ was synthesized according to a literature procedure.[53]

CoralPor tips were purchased from CH Instruments (Bee Cave, TX, USA) and used to prepare a Ag/Ag^+ reference electrode according to the protocol obtained from BASi;[55] 10× phosphate-buffered saline (PBS) was purchased from Seracare (Milford, MA, USA) and diluted to 1× to obtain a 0.1 M PBS buffer (150 mM NaCl, 10 mM sodium phosphate, pH 7.4). A previously reported adenosine aptamer[1] including a 5′ extension, a 5′ amine terminus, and a 3′ fluorescein amidite (FAM) label and a scrambled version of the same oligonucleotide sequence as the aptamer ("scrambled control") were purchased from Integrated DNA Technologies (Coralville, IA, USA). The sequences of the aptamer and scrambled control are as follows.

Adenosine aptamer: 5′-/5AmMC6/AAA AAC ACT GAC CTG GGG GAG TAT TGC GGA GGA AGG T/36-FAM/-3′.

Scrambled control: 5′- /5AmMC6/AAA AAG GCG AGT ATG TAA GCG TGC GGC GAT GAT GGA C/36-FAM/-3′.

Adenosine was purchased from Calbiochem (San Diego, CA, USA). Uridine-5-triphosphate was purchased from Chem-Impex (Wood Dale, IL, USA). Cytosine was purchased from Beantown Chemical (Hudson, NH, USA). Guanosine-5-triphosphate was purchased from MP Biochemicals (Irvine, CA, USA). Ultrapure deionized (DI) water was obtained from a Millipore Direct Q system (18.2 MΩ·cm). All reagents were used as received unless specifically stated otherwise. Water, solutions, and supplies utilized with the aptamer were sterile or autoclaved before use.

2.2. Instrumentation. All electrochemical measurements were performed using CV on a Pine WaveNow potentiostat. The setup consisted of a three-electrode system. The working electrode was an ITO-coated glass slide. The reference electrode was either a Ag/Ag^+ electrode for electropolymerization in acetonitrile or a Ag/AgCl electrode for aqueous polymer electrochemistry and sensing. A platinum flag was used as a counter electrode. All CV measurements were performed at a scan rate of 100 mV/s unless otherwise stated.

Contact angle measurement were taken by a ramé-hart model 200-F1 goniometer equipped with DROPimage software. Ten microliter drops of DI water were pipetted onto each sample for characterization of the contact angle. A fluorescence microscope (Invitrogen EVOS FL digital fluorescence microscope) was utilized to obtain fluorescence images of the immobilized aptamer using the green fluorescent protein (GFP)

https://doi.org/10.1021/acsapm.1c01348
ACS Appl. Polym. Mater. 2021, 3, 6674−6683

Scheme 1. Schematic Illustration of the Preparation of the Adenosine Aptasensor[a]

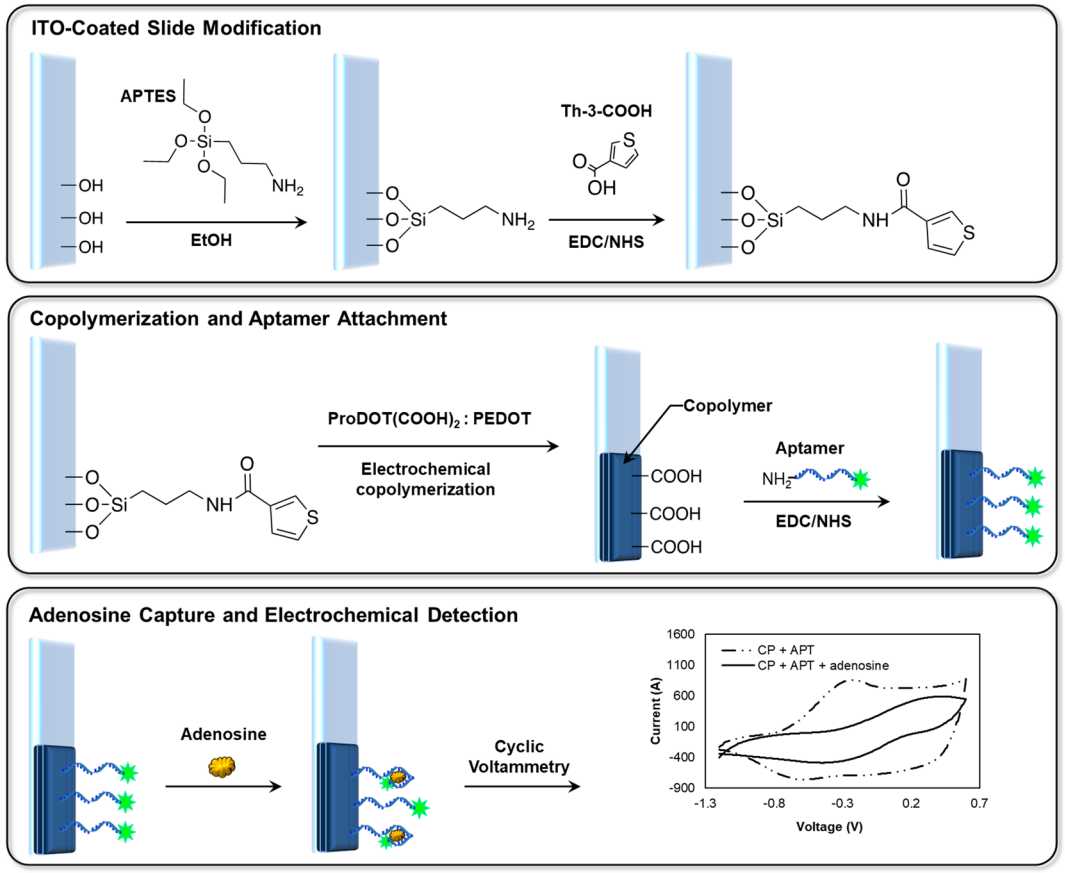

[a]CP = conducting polymer, APT = aptamer.

filter cube of the microscope (λ_{EX} = 470 nm, λ_{EM} = 525 nm). The images were captured at a light intensity of 50%, shutter speed of 1 ns, and 40× magnification. The fluorescence of the aptamer-functionalized biosensors was obtained by wetting the sample with 0.1 M PBS prior to imaging.

2.3. Fabrication of the Aptasensor. The fabrication of the adenosine aptasensor is outlined in Scheme 1. ITO-coated glass slides were used as substrates for aptasensor fabrication. These slides were pretreated to enhance coating stability as follows. First, the ITO-coated slide was cleaned to improve the presence of hydroxyl groups on the surface. For this purpose, the ITO-coated glass was soaked in 1 M HCl for 10 s; it was then washed immediately with DI water followed by an acetone wash. Next, amine groups were introduced to the surface of the ITO-coated glass by immobilizing APTES on the ITO-coated glass by a silanization protocol published by Thermo Scientific.[56] An APTES solution (2% in EtOH, 75 mL) was pipetted on the precleaned ITO-coated glass surface and incubated for 10 min. The surface was washed with EtOH (10 × 100 mL) and dried under argon. Finally, covalent modification of the surface was accomplished by conjugation of 3-Th-COOH using carbodiimide chemistry to improve the attachment of the CP to the substrate. An aqueous solution of 0.16 M EDC/0.26 M NHS (100 mL) containing 0.1 M 3-Th-COOH was pipetted on the surface of the APTES-modified ITO-coated slide and allowed to react for 1 h. The slide was rinsed with DI water (10 × 100 mL) and dried under argon.

The pretreated slides were used for polymer deposition as follows. The 3-Th-COOH-modified electrode was inserted as a working electrode into an acetonitrile solution containing 0.1 M TBAP, 0.01 M ProDOT−$(COOH)_2$, and 0.005 M EDOT in a three-electrode electrochemical setup with a Ag/Ag^+ reference electrode and a platinum flag as the counter electrode. A potential sweep between −1.2 and 1.7 V was applied for 3 cycles to obtain the copolymer. The electrochemical behavior of the copolymer was then characterized in 0.1 M PBS with a potential sweep from −1.2 to 0.6 V and a Ag/AgCl reference electrode. The −COOH-functionalized copolymer was then incubated with an aqueous solution of EDC/NHS (0.16 M EDC/0.26 M NHS, 100 mL) containing 30 mM aptamer or control oligonucleotide for 2.5 h. The resulting aptasensor was washed extensively with PBS to remove excess aptamer or control oligonucleotide from the electrode surface. The contact angle for each modification step was measured. The successful immobilization of the fluorescently labeled aptamer was also confirmed using fluorescence microscopy and cyclic voltammetry with a potential sweep from −1.2 to 0.6 V in 0.1 M PBS and with a Ag/AgCl reference electrode.

2.4. Detection of Adenosine. The aptasensor was incubated with solutions of adenosine at increasing concentrations from 96 pM to 3000 mM in 0.1 M PBS (pH 7.4). For each measurement, the aptasensor was incubated in the adenosine solution for 30 min. The adenosine-bound aptasensor was characterized using CV from −1.2 to 0.6 V in 0.1 M PBS with a Ag/AgCl reference electrode to determine its analytic performance. CVs were repeated three times after exposure to each adenosine concentration. The average current response for the three measurements is reported.

2.5. Selectivity, Specificity, Reusability, and Storage Stability Studies. The selectivity of the aptasensor was investigated by evaluating the sensor's response upon interaction to interfering molecules that should not be recognized by the adenosine aptamer. The selected molecules were the nucleoside cytosine and the nucleotides guanosine 5′-triphosphate (GTP) and uridine 5′-triphosphate (UTP). The interference of the various nucleotides was tested by incubating the aptasensor with adenosine in the presence of an interfering nucleoside/nucleotide mixture. The specificity of the aptasensor was investigated using the previously mentioned scrambled control, which should not be specific for adenosine.

https://doi.org/10.1021/acsapm.1c01348
ACS Appl. Polym. Mater. 2021, 3, 6674−6683

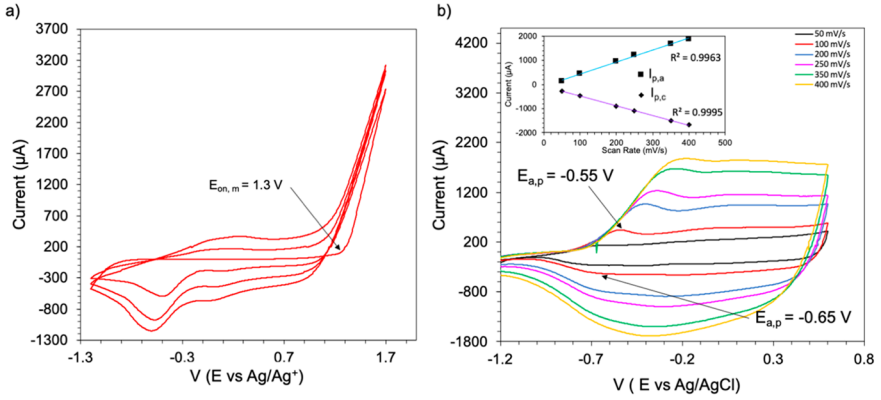

Figure 1. Cyclic voltammetry plots of (a) PProDOT−$(COOH)_2$:PEDOT copolymer growth (0.01 M:0.005 M monomer ratio in 0.1 M TBAP/acetonitrile at a scan rate of 100 mV/s) and (b) copolymer cycling and scan rate dependence (inset) in 0.1 M PBS (pH 7.4).

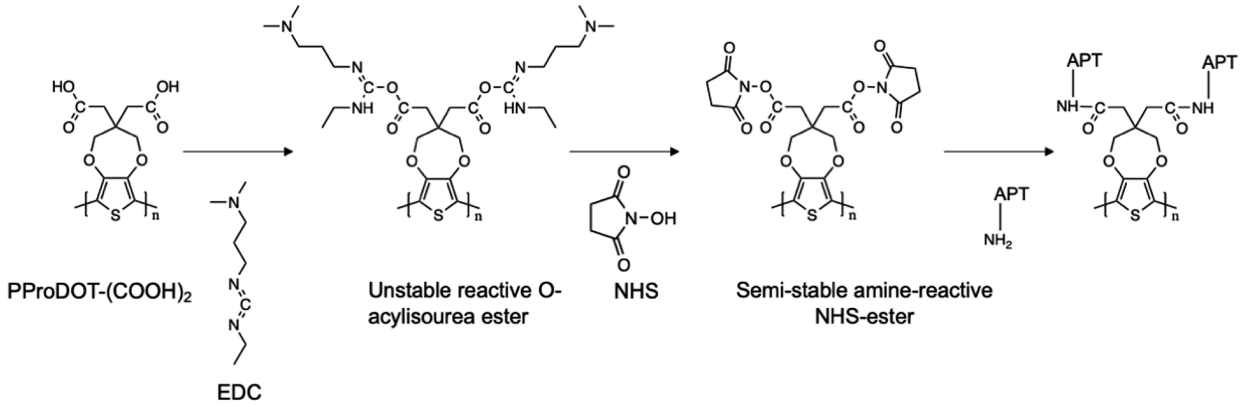

Figure 2. EDC/NHS coupling reaction for aptamer immobilization on the copolymer surface.

Reusability was determined by incubating the aptasensor in adenosine and regenerating the used aptasensor by incubating in excess 0.1 M PBS and heating to 92 °C to cause thermal denaturing of the aptamer. The regenerated aptasensor was then reincubated in adenosine solution. The CV measurement was obtained after each regeneration step.

The storage stability of the aptasensor was investigated by incubating the aptasensor in 0.1 M PBS (pH 7.4) or in the dry state under argon for a period of 7 days. CV measurements of these aptasensors were obtained every 2 days.

2.6. Statistical Analysis. All electrochemical measurements were obtained in triplicate. The obtained data were reported as mean values ± standard deviation (SD). A 2-sample equal variance *t* test was performed to analyze the statistical significance between data groups and the respective controls. $^*p < 0.05$ was set as the significance level.

3. RESULTS AND DISCUSSION

3.1. Copolymer Development and Characterization. ProDOT−$(COOH)_2$ was first electropolymerized onto ITO-coated glass slides, and the resultant PProDOT−$(COOH)_2$ homopolymer films were investigated for use as aptasensors. The films were found to be unstable in slightly basic solutions such as buffer because they converted to the water-soluble carboxylate salt; a similar behavior for an asymmetric, monoacid-functionalized PProDOT was reported by Mantione et al.[54] Solubility in buffer led to serious delamination problems in PBS (Figure S1).

In order to prevent solubility-induced delamination in mildly basic buffer solutions, a ProDOT−$(COOH)_2$:EDOT copolymer (2:1 ratio of ProDOT−$(COOH)_2$:EDOT) was electrochemically polymerized on 3-Th-COOH-modified, ITO-coated glass using cyclic voltammetry. The potential window utilized for the electrochemical growth was from −1.2 to 1.7 V. The copolymerization was possible because of the relatively close potential for the onset of monomer oxidation of each of the two monomers. EDOT and ProDOT−$(COOH)_2$ exhibit onsets of monomer oxidation at 1.3 and 1.4 V, respectively, and the resulting copolymer has a monomer oxidation onset potential ($E_{on,m}$) of 1.3 V (Figure 1a). The copolymer exhibits an anodic peak potential ($E_{a,p}$) of −0.55 V and a cathodic peak potential ($E_{c,p}$) of −0.65 V at a scan rate of 100 mV/s (Figure 1b).

In order to confirm that the copolymer was stably immobilized on the electrode, the copolymer electrochemistry was studied over a wide range of scan rates (Figure 1b); the inset in Figure 1b shows the resulting scan rate dependence obtained from the peak anodic and cathodic current at each scan rate. The linear response between the peak current and the scan rate of the copolymer in the PBS buffer suggests that the copolymer is electroactive and adhered to the electrode, as governed by the theory of surface-immobilized redox centers[57,58] where the peak current (i_p) is given by the following equation (eq 1)

$$i_p = \frac{n^2F^2\Gamma\upsilon}{4RT} \quad (1)$$

where Γ is the total amount of reactant initially present at the electrode surface (moles), *F* is Faraday's constant (Coulombs/mol), υ is the scan rate (V/s), *n* is the number of electrons transferred per mole of product, *R* is the gas constant, and *T* is the absolute temperature (K).

3.2. Aptamer Immobilization and Characterization. The aptamer was immobilized on the copolymer surface via an

https://doi.org/10.1021/acsapm.1c01348
ACS Appl. Polym. Mater. 2021, 3, 6674−6683

amide bond formed from the activation of the carboxylic acid groups on the CP with EDC and NHS to create a semistable amine-reactive ester, which allows for efficient conjugation to the amine-terminated aptamer. Figure 2 shows the reaction chemistry of the aptamer attachment to the copolymer. EDC activates carboxylic acid groups and forms an amine-reactive *O*-acylisourea intermediate that is unstable in aqueous solutions.[59] Subsequently, NHS couples to the activated carboxylic acid groups and forms a semistable NHS ester that allows for efficient conjugation to primary amines. The successful immobilization of the aptamer was confirmed by fluorescence microscopy. The presence of a FAM fluorophore at the 3′ of the aptamer resulted in green fluorescence of the successfully bound aptamer onto the CP (Figure S2).

Contact angle measurements provide information about the interaction of water with the different functional groups and the characteristic hydrophilic nature on the modified ITO-coated glass surface. Contact angle measurements were taken to observe the change in the hydrophobic/hydrophilic nature of the electrode surface at each modification step due to changes in the surface chemistry as seen in Figure 3.

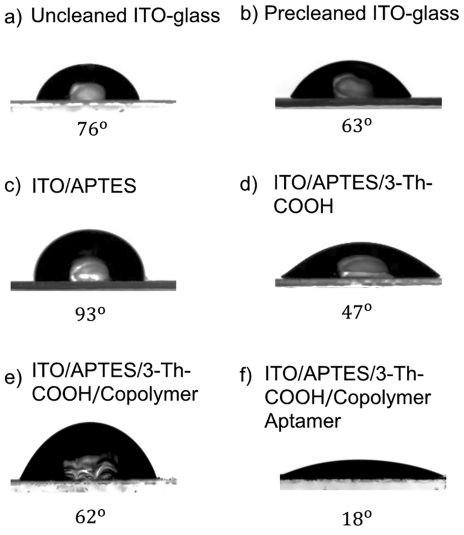

Figure 3. Contact angle measurements of (a) untreated and (b–f) modified ITO-coated glass substrates.

The as-purchased uncleaned ITO-coated slides are expected to be contaminated with organic matter and have a lower presence of hydroxyl groups;[60] as a result, the corresponding contact angle was 76°. The contact angle was reduced to 63° after the precleaning step was done, which suggests the availability of more hydrophilic hydroxyl groups on the ITO-coated glass' surface. The silanization step, which introduces APTES to the surface, makes the surface more hydrophobic, as confirmed by the corresponding increase in the contact angle of the electrode to 94°. The introduction of 3-Th-COOH to the surface made for a more hydrophilic nature, resulting in a corresponding reduction in the contact angle to 48°. After electropolymerization, the contact angle increased to 62°, suggesting it is still hydrophilic but less hydrophilic than the 3-Th-COOH-modified surface. Attachment of the aptamer resulted in a sharp increase in hydrophilicity with a reduction of the contact angle to 18°.

The aptasensor was characterized electrochemically by investigating the change in electrochemical response of the CP occurring during cyclic voltammetry after each fabrication step. The CV measurements were obtained from a potential window from −1.2 to 0.6 V at a scan rate of 100 mV/s in 0.1 M PBS (pH 7.4). The CP CV (Figure 4) shows two oxidation potentials at −0.66 and 0.1 V. These peaks shifted to become one broad peak at −0.25 V with a corresponding increase in the electrochemical response by 400 mA after immobilization of the aptamer on the surface. The binding of adenosine to the aptasensor resulted in a reduction in the current response, potentially due to the conformational change of the aptamer associated with the formation of the aptamer–target complex,[1] which could interfere with the flow of electrons from the PBS solution to the surface of the CP. The presence of the negatively charged aptamer and the captured adenosine could hinder the charge transfer from the solution to the electroactive polymer, thereby causing a decrease in the peak current response of the aptasensor. The shift to higher oxidation potential ($E_{a,p}$ = 0.3 V) may be due to a reduction in the conductivity in the presence of adenosine, requiring a higher potential difference to cause current to flow through to the surface of the conducting polymer.

3.3. Detection of Adenosine. The aptasensor was incubated with adenosine solutions at various concentrations (from 96 pM to 3000 mM) and characterized using CV with a potential window from −1.2 to 0.6 V in 0.1 M PBS. As observed

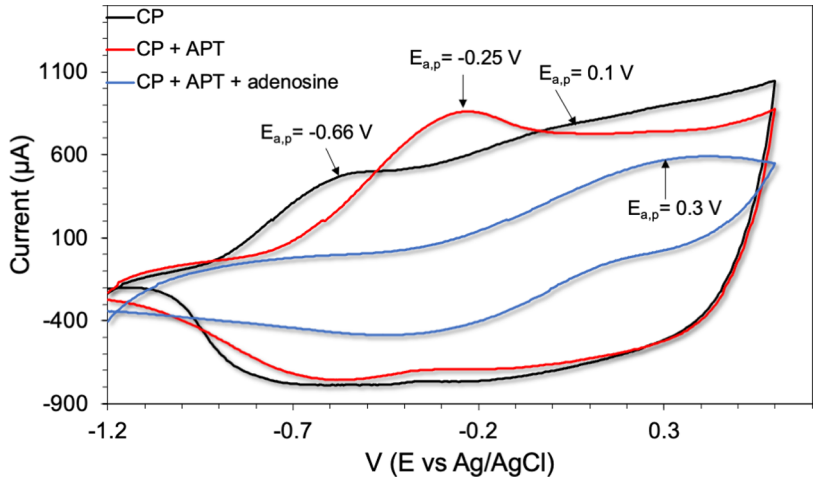

Figure 4. Cyclic voltammograms of CP, CP+APT, and CP+APT+adenosine at a scan rate of 100 mV/s in 0.1 M PBS (pH 7.4). APT = Aptamer.

https://doi.org/10.1021/acsapm.1c01348
ACS Appl. Polym. Mater. 2021, 3, 6674–6683

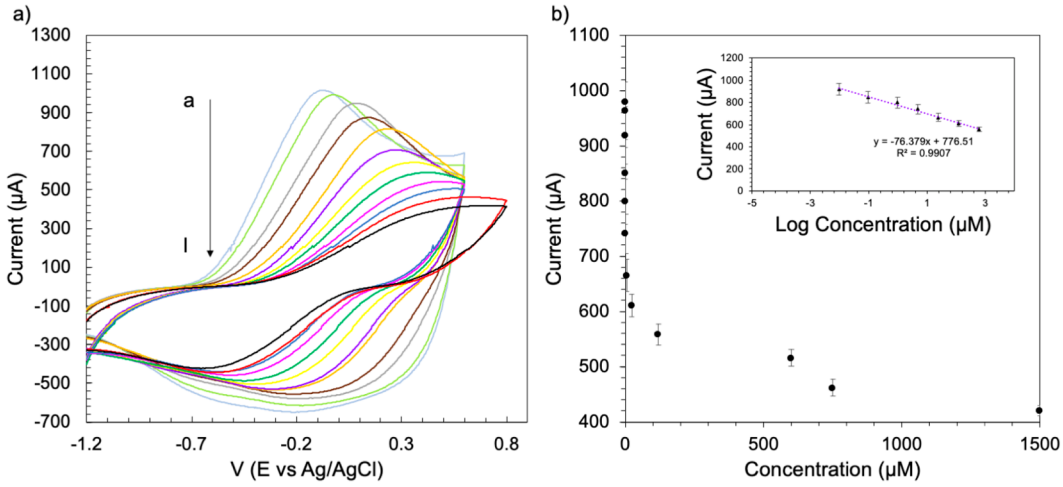

Figure 5. (a) Electrochemical response: CV of the aptasensor after incubation with an increasing concentration of adenosine from *a* to l (96 pM, 960 pM, 9.6 nM, 96 nM, 960 nM, 4.8 μM, 24 μM, 120 μM, 600 μM, 750 μM, 1500 μM, and 3000 μM) in 0.1 M PBS (pH 7.4). (b) Plot of the biosensor response as a function of adenosine concentration ((inset) linear plot of the peak current vs log of the adenosine concentration in the range from 9.6 nM to 600 mM). Error bars represent the standard deviation of three measurements.

Scheme 2. Comparison of the Electrochemical Aptasensor Performance[a]

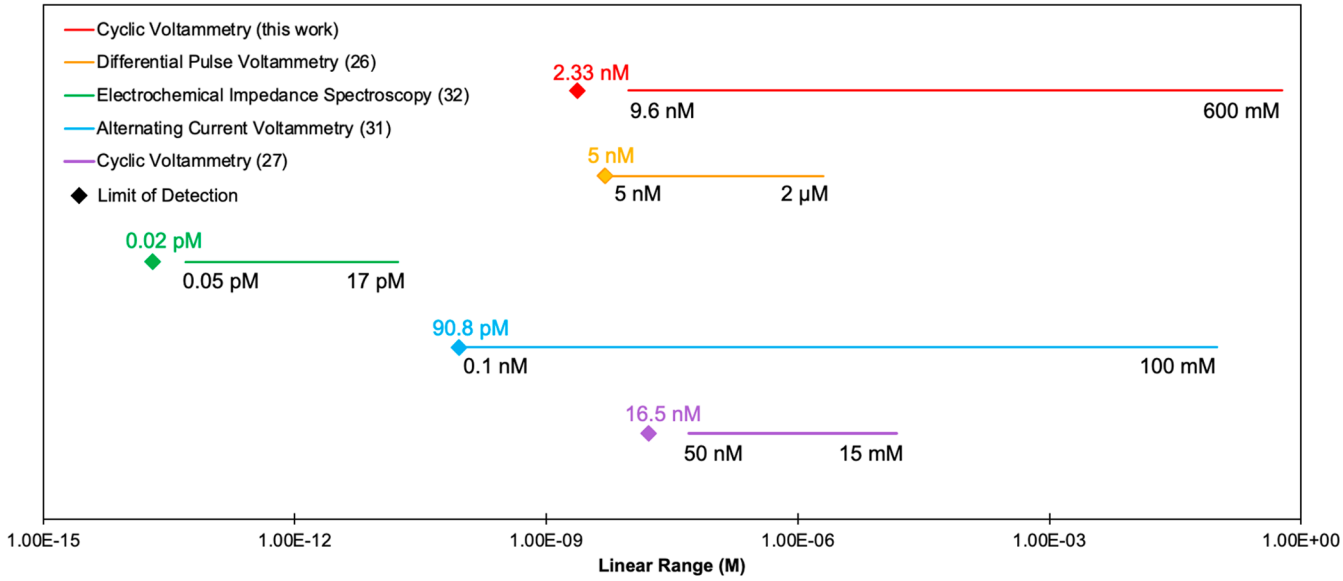

[a]Reference numbers for each article are provided in parentheses next to the data legend.

in Figure 5a, a decrease in the peak electrochemical current response and a shift to higher oxidation potentials were observed with increasing analyte concentration. This phenomenon has been observed in other aptasensors[27,61,62] and has been attributed to the binding of bulky analyte species to the polymer.[61] The bound analyte increases steric bulk, which introduces resistance to the structural changes that accompany oxidation, increasing the oxidation potential. The bulky analyte also inhibits counterion migration into the film, decreasing the current response. Figure 5b shows a plot of the electrochemical response vs concentration with an inset that shows the region of the concentration that is linear within the wide range from 9.6 nM to 600 mM. The limit of detection (LOD) of the aptasensor is 2.33 nM as calculated from the formula[63]

$$x_{\mathrm{LOD}} = \frac{K \times SD}{m} \qquad (2)$$

where x_{LOD} is the limit of detection on a log scale calculated from the linear plot, *SD* is the standard deviation of the current response of the blank measurements, *m* is the slope of the linear equation, and *K* is the numeric value chosen according to the confidence level desired; our calculations use $K = 3$, which is consistent with the literature.[63] The obtained results suggest a highly sensitive platform for the detection of adenosine with a wide linear range. A comparison of the analytical performance of the aptasensor with other adenosine aptasensors previously reported in the literature is given in Scheme 2.

It is worth noting that control studies were conducted in which the aptasensor was monitored over time when in adenosine-free buffer (Figure S3) and in which a biosensor containing the CP but without the aptamer was exposed to solutions of varying adenosine concentration (Figure S4). Both control studies showed an increased current response, in contrast to the result observed for the aptasensor (Figure 5).

https://doi.org/10.1021/acsapm.1c01348
ACS Appl. Polym. Mater. 2021, 3, 6674−6683

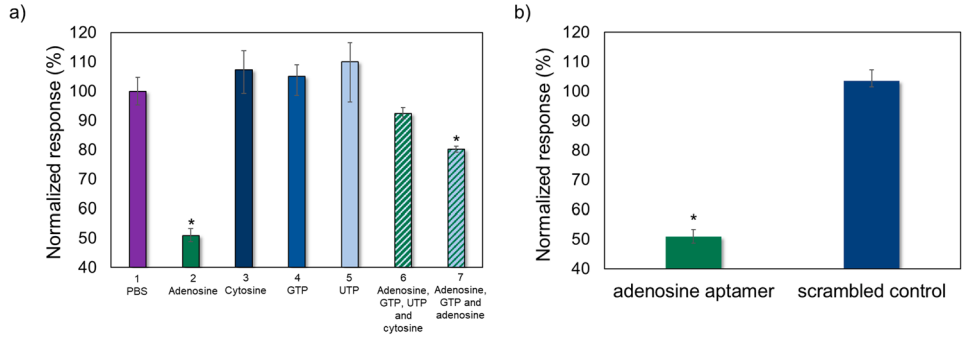

Figure 6. (a) Selectivity study of the aptasensor. Bars 2−5 and 7 were obtained using solutions that were 3 mM in each analyte, while bar 6 used a solution that was 300 μM adenosine and 30 μM of each interfering nucleoside/nucleotide. (b) Specificity study of the aptasensor with a scrambled oligonucleotide control strand. Normalized response refers to the response of the sensor upon interaction with 3 mM adenosine relative to that of the biosensor response in PBS. * $p < 0.05$ relative to the sensor incubated in PBS.

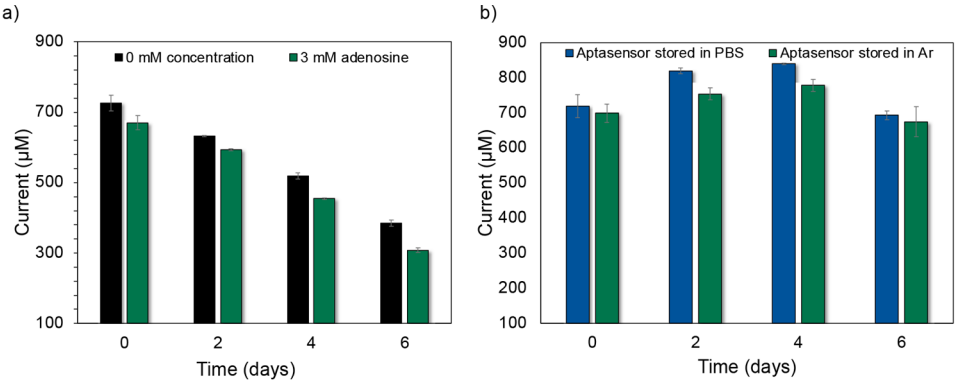

Figure 7. (a) Current response of the aptasensor with adenosine detection, regeneration, and storage. (b) Aptasensor storage in PBS and in dry storage under argon.

The performance of this aptasensor is comparable with other previously reported electrochemical adenosine aptasensors. The obtained LOD of our aptasensor outperforms similar aptasensors reported by Liu et al.[27] and Sun et al.[26] with reported LODs of 16.5 and 5 nM, respectively. The linear range obtained from our aptasensor was much wider than that of previously reported aptasensors based on cyclic voltammetry, differential pulse voltammetry, and electrochemical impedance spectroscopy (Scheme 2), and it was comparable to that of an alternating current voltametric aptasensor. The aptasensor in this work also provides an opportunity for a label-free method of detection, which may make it less expensive than other labeled biosensors.

3.4. Selectivity Studies. The selectivity of the aptasensor was evaluated by comparing its change in peak current response in the presence of adenosine to that upon interaction with the interfering nucleosides and nucleotides cytosine, GTP and UTP individually, as well as a mixture. The normalized change in electrochemical response was plotted for all of the samples. As can be seen in Figure 6a, the current response of the aptasensor in 3 mM of each of the interfering nucleotides showed no significant change relative to the initial aptasensor response to buffer (labeled aptasensor), while the response of the aptasensor to 3 mM adenosine resulted in the expected and statistically significant change in current. Incubation of the aptasensor in a mixture of 300 mM adenosine and 30 mM each of the interfering nucleosides/nucleotides (cytosine, GTP, and UTP) yielded a current response that was statistically unchanged from that of the bare aptasensor in buffer. This is possibly explained by interaction of adenosine with uridine through hydrogen bonding and other noncovalent interactions, causing poor detection of adenosine in the solution.[64] The exclusion of UTP and subsequent detection of 3 mM adenosine in the presence of 3 mM each of cytosine and GTP resulted in a statistically significant change in the current response as observed in Figure 6a.

Figure 6b shows the specificity study of the aptasensor against a sensor prepared with the scrambled control. The sensor including the scrambled control had no reduction in normalized current response when exposed to 3 mM adenosine relative to its response in PBS, which suggests that the scrambled control is not specific and does not possess the affinity to form an aptamer−target complex like the adenosine-specific aptasensor.

3.5. Reusability and Storage Stability Studies. For the reusability studies, the aptasensor was tested by CV in 0.1 M PBS buffer and after incubation in 3 mM adenosine for 30 min. After sensing, the sensor was regenerated and stored in 0.1 M PBS buffer prior to storage for 2 days and retesting in buffer and after reincubation in adenosine. This process was repeated for a total of 6 days. Figure 7a shows the peak current response of the sensor before and after adenosine detection. The current response decreased to 87% of the original current response at day 0 by day 2 and 52% by day 6. However, the percent change in current response in the presence of adenosine relative to that in buffer was not statistically different for up to 2 days (Figure S5). This suggests the aptasensor can be used up to 2 times if properly stored and regenerated after use.

A second study investigated the storage stability of the sensor prior to use. The aptasensor was stored at room temperature in

https://doi.org/10.1021/acsapm.1c01348
ACS Appl. Polym. Mater. 2021, 3, 6674−6683

0.1 M PBS, and the CV was measured in PBS after each storage interval of 2 days. The aptasensor was not exposed to adenosine in these studies. Figure 7b shows the response of the aptasensor in PBS storage and dry storage under argon over a period of 6 days. The data from the PBS storage demonstrates that there was no significant decrease in sensor current over a period of 6 days. In fact, the aptasensor retained 96% of its electroactivity after the 6-day period, which suggest good electrochemical stability.

Finally, the electrochemical stability of the aptasensor was also investigated in dry storage under argon. This was particularly of interest because it represents a more commercially preferable storage condition for the aptasensor. Similar to the aptasensor storage in PBS, the aptasensor showed no significant reduction in the electrochemical response after a 6-day storage period. The electrochemical response of the aptasensor decreased by 3% after 6 days, which suggests good electrochemical stability.

4. CONCLUSIONS

A sensitive and selective aptasensor was successfully developed for the detection of adenosine. The PProDOT−$(COOH)_2$ homopolymer was not electrochemically stable and delaminated in PBS buffer due to its conversion to its more water-soluble salt form. This led to the investigation of an alternative method to improve the properties of the polymer and also the adhesion of the polymer to the electrode. The optimized results of those experiments gave rise to utilizing a copolymer of EDOT and ProDOT−$(COOH)_2$ in addition to modifying the ITO-coated glass slide with a small molecule to serve as a nucleation point during the electrochemical copolymerization. Copolymerization yielded an insoluble film for aptamer attachment and allowed for the detection of adenosine binding events through a label-free means by measuring the electrochemical response of the CP at each modification step and detection step. The adenosine aptasensor possessed a wide linear range from 9.6 nM to 600 mM and a low LOD of 2.33 pM. The success of the conducting copolymer-based system provides an opportunity for a sensitive electrochemical detection platform that can be utilized for detecting other disease-specific biomarkers. Future experiments will investigate the applicability of aptasensors that utilize the same polymer signal transducers for the detection of pathological biomarkers in clinically relevant samples.

■ ASSOCIATED CONTENT

Supporting Information

The Supporting Information is available free of charge at https://pubs.acs.org/doi/10.1021/acsapm.1c01348.

Detailed description, analysis, and figures associated with conductive polymer adhesion improvement strategy; confirmation of aptamer attachment by fluorescence microscopy; controls for biosensor response; and aptasensor reusability (PDF)

■ AUTHOR INFORMATION

Corresponding Authors

Tania Betancourt − *Materials Science, Engineering and Commercialization Program and Department of Chemistry and Biochemistry, Texas State University, San Marcos, Texas 78666, United States;* orcid.org/0000-0002-2460-6133; Email: tania.betancourt@txstate.edu

Jennifer A. Irvin − *Materials Science, Engineering and Commercialization Program and Department of Chemistry and Biochemistry, Texas State University, San Marcos, Texas 78666, United States;* orcid.org/0000-0003-3500-8419; Email: jennifer.irvin@txstate.edu

Authors

Damilola O. Runsewe − *Materials Science, Engineering and Commercialization Program, Texas State University, San Marcos, Texas 78666, United States;* Present Address: Manufacturing, Technology and Engineering, Corning Incorporated, Corning, New York 14831, United States; orcid.org/0000-0003-1813-9732

Grace Haya − *Department of Chemistry and Biochemistry, Texas State University, San Marcos, Texas 78666, United States;* orcid.org/0000-0003-0498-2446

Complete contact information is available at: https://pubs.acs.org/10.1021/acsapm.1c01348

Author Contributions

The manuscript was written through contributions of all authors. All authors have given approval to the final version of the manuscript.

Funding

This research was funded by the National Science Foundation (NSF) Partnership for Research and Education in Materials, grant no. 2122041, the NSF Research Experiences for Undergraduates grant no. 1757843, and a Texas State University Doctoral Research Fellowship.

Notes

The authors declare no competing financial interest.

■ ACKNOWLEDGMENTS

The authors thank Dr. William Brittain for use of his contact angle analyzer and Ms. Kelli Burke and Mr. Gabriel Pohlman for helpful discussions.

■ ABBREVIATIONS

APT, aptamer; APTES, (3-aminopropyl)triethoxysilane; ATP, adenosine triphosphate; CCL2, CC chemokine ligand 2; CCR2, CC chemokine receptor 2; CCR5, CC chemokine receptor 5; CP, conducting polymer; CV, cyclic voltammetry; DI, deionized; $E_{a,p}$, anodic peak potential; $E_{c,p}$, cathodic peak potential; $E_{on,m}$, monomer oxidation onset potential; EDC, 1-ethyl-3-(3-(dimethylamino)propyl)carbodiimide; EDOT, 3,4-ethylenedioxythiophene; EtOH, ethanol; FAM, 3′-fluorescein amidite; GFP, green fluorescence protein; GTP, guanosine 5′-triphosphate; HCl, hydrochloric acid; ITO, indium tin oxide; LOD, limit of detection; NHS, *N*-hydroxysuccinimide; NMR, nuclear magnetic resonance; PBS, phosphate-buffered saline; PEDOT, poly(3,4-ethylenedioxythiophene); PProDOT−$(COOH)_2$, poly(2,2′-(3,4-dihydro-2*H*-thieno[3,4-*b*][1,4]-dioxepine-3,3-diyl)diacetic; PProDOT, poly(3,4-propylene-dioxythiophene); ProDOT−$(COOH)_2$, 2*H*-thieno[3,4-*b*]-[1,4]dioxepin-3,3(4*H*)-diacetic acid; SD, standard deviation; SELEX, systematic evolution of ligands using exponential enrichment; TBAP, tetrabutylammonium perchlorate; 3-Th-COOH, 3-thiophenecarboxylic acid; TLC, thin layer chromatography; UTP, uridine 5′-triphosphate

■ REFERENCES

(1) Huizenga, D. E.; Szostak, J. W. A DNA Aptamer That Binds Adenosine and ATP. *Biochemistry* **1995**, *34*, 656−665.

(2) Zhao, Y.; Tan, L.; Gao, X.; Jie, G.; Huang, T. Silver Nanoclusters-Assisted Ion-Exchange Reaction with CdTe Quantum Dots for

Photoelectrochemical Detection of Adenosine by Target-Triggering Multiple-Cycle Amplification Strategy. *Biosens. Bioelectron.* **2018**, *110*, 239−245.
(3) Li, W.; Sun, J.; Wang, H.; Wang, L.; Jiang, W. Multifunctional Aptamer Probe Mediated Cascade Amplification for Label-Free Detection of Adenosine. *Sens. Actuators, B* **2018**, *260*, 581−586.
(4) Qiang, W.; Wang, X.; Li, W.; Chen, X.; Li, H.; Xu, D. A Fluorescent Biosensing Platform Based on the Polydopamine Nanospheres Intergrating with Exonuclease III-Assisted Target Recycling Amplification. *Biosens. Bioelectron.* **2015**, *71*, 143−149.
(5) Huang, D. W.; Niu, C. G.; Zeng, G. M.; Ruan, M. Time-Resolved Fluorescence Biosensor for Adenosine Detection Based on Home-Made Europium Complexes. *Biosens. Bioelectron.* **2011**, *29*, 178−183.
(6) Headrick, J. P.; Ashton, K. J.; Rose'Meyer, R. B.; Peart, J. N. Cardiovascular Adenosine Receptors: Expression, Actions and Interactions. *Pharmacol. Ther.* **2013**, *140* (1), 92−111.
(7) Wang, Z.; Zang, R.; Niu, Z.; Wang, W.; Wang, X.; Tang, Y. Synthesis and Antiviral Effect of Phosphamide Modified Vidarabine for Treating HSV 1 Infections. *Bioorg. Med. Chem. Lett.* **2021**, *52*, 128405.
(8) Procopio, M. C.; Lauro, R.; Nasso, C.; Carerj, S.; Squadrito, F.; Bitto, A.; Di Bella, G.; Micari, A.; Irrera, N.; Costa, F. Role of Adenosine and Purinergic Receptors in Myocardial Infarction: Focus on Different Signal Transduction Pathways. *Biomedicines* **2021**, *9* (2), 204.
(9) Johnson, T. A.; Jinnah, H. A.; Kamatani, N. Shortage of Cellular ATP as a Cause of Diseases and Strategies to Enhance ATP. *Front. Pharmacol.* **2019**, *10*, 98.
(10) Martins, I.; Wang, Y.; Michaud, M.; Ma, Y.; Sukkurwala, A. Q.; Shen, S.; Kepp, O.; Métivier, D.; Galluzzi, L.; Perfettini, J. L.; Zitvogel, L.; Kroemer, G. Molecular Mechanisms of ATP Secretion during Immunogenic Cell Death. *Cell Death Differ.* **2014**, *21*, 79−91.
(11) Tuerk, C.; Gold, L. Systematic Evolution of Ligands by Exponential Enrichment: RNA Ligands to Bacteriophage T4 DNA Polymerase. *Science (Washington, DC, U. S.)* **1990**, *249* (4968), 505−510.
(12) Ellington, A. D.; Szostak, J. W. In Vitro Selection of RNA Molecules That Bind Specific Ligands. *Nature* **1990**, *346* (1), 818−832.
(13) Lv, S.; Zhang, K.; Zhu, L.; Tang, D. Zif-8-Assisted Nayf4:Yb,Tm@zno Converter with Exonuclease Iii-Powered Dna Walker for near-Infrared Light Responsive Biosensor. *Anal. Chem.* **2020**, *92*, 1470−1476.
(14) Zeng, R.; Luo, Z.; Su, L.; Zhang, L.; Tang, D.; Niessner, R.; Knopp, D. Palindromic Molecular Beacon Based Z-Scheme BiOCl-Au-CdS Photoelectrochemical Biodetection. *Anal. Chem.* **2019**, *91* (3), 2447−2454.
(15) Villalonga, A.; Pérez-Calabuig, A. M.; Villalonga, R. Electrochemical Biosensors Based on Nucleic Acid Aptamers. *Anal. Bioanal. Chem.* **2020**, *412*, 55−72.
(16) Zou, X.; Wu, J.; Gu, J.; Shen, L.; Mao, L. Application of Aptamers in Virus Detection and Antiviral Therapy. *Front. Microbiol.* **2019**, *10*, 1462.
(17) Li, F.; Yu, Z.; Han, X.; Lai, R. Y. Electrochemical Aptamer-Based Sensors for Food and Water Analysis: A Review. *Anal. Chim. Acta* **2019**, *1051*, 1−23.
(18) Campuzano, S.; Yaez-Sedeno, P.; Pingarron, J. Electrochemical Affinity Biosensors in Food Safety. *Chemosensors* **2017**, *5*, 8.
(19) Campuzano, S.; Yáñez-Sedeño, P.; Pingarrón, J. M. Electrochemical Affinity Biosensors Based on Selected Nanostructures for Food and Environmental Monitoring. *Sensors* **2020**, *20*, 5125.
(20) Takaloo, S.; Moghimi Zand, M. Wearable Electrochemical Flexible Biosensors: With the Focus on Affinity Biosensors. *Sens. Bio-Sensing Res.* **2021**, *32*, 100403.
(21) Campuzano, S.; Yanez-Sedeno, P.; Pingarron, J. Molecular Biosensors for Electrochemical Detection of Infectious Pathogens in Liquid Biopsies: Current Trends and Challenges. *Sensors* **2017**, *17*, 2533.
(22) Runsewe, D.; Betancourt, T.; Irvin, J. Biomedical Application of Electroactive Polymers in Electrochemical Sensors: A Review. *Materials* **2019**, *12*, 2629.
(23) Zhang, Y. L.; Huang, Y.; Jiang, J. H.; Shen, G. L.; Yu, R. Q. Electrochemical Aptasensor Based on Proximity-Dependent Surface Hybridization Assay for Single-Step, Reusable, Sensitive Protein Detection. *J. Am. Chem. Soc.* **2007**, *129*, 15448−15449.
(24) Bao, T.; Shu, H.; Wen, W.; Zhang, X.; Wang, S. A Sensitive Electrochemical Aptasensor for ATP Detection Based on Exonuclease III-Assisted Signal Amplification Strategy. *Anal. Chim. Acta* **2015**, *862*, 64−69.
(25) Kashefi-Kheyrabadi, L.; Mehrgardi, M. A. Aptamer-Conjugated Silver Nanoparticles for Electrochemical Detection of Adenosine Triphosphate. *Biosens. Bioelectron.* **2012**, *37*, 94−98.
(26) Sun, C.; Liu, X.; Feng, K.; Jiang, J.; Shen, G.; Yu, R. An Aptazyme-Based Electrochemical Biosensor for the Detection of Adenosine. *Anal. Chim. Acta* **2010**, *669*, 87−93.
(27) Liu, Z.; Yuan, R.; Chai, Y.; Zhuo, Y.; Hong, C.; Yang, X.; Su, H.; Qian, X. Highly Sensitive, Reusable Electrochemical Aptasensor for Adenosine. *Electrochim. Acta* **2009**, *54*, 6207−6211.
(28) Zhang, S.; Xia, J.; Li, X. Electrochemical Biosensor for Detection of Adenosine Based on Structure-Switching Aptamer and Amplification with Reporter Probe DNA Modified Au Nanoparticles. *Anal. Chem.* **2008**, *80*, 8382−8388.
(29) Santos-Cancel, M.; Simpson, L. W.; Leach, J. B.; White, R. J. Direct, Real-Time Detection of Adenosine Triphosphate Release from Astrocytes in Three-Dimensional Culture Using an Integrated Electrochemical Aptamer-Based Sensor. *ACS Chem. Neurosci.* **2019**, *10*, 2070−2079.
(30) Sanghavi, B. J.; Sitaula, S.; Griep, M. H.; Karna, S. P.; Ali, M. F.; Swami, N. S. Real-Time Electrochemical Monitoring of Adenosine Triphosphate in the Picomolar to Micromolar Range Using Graphene-Modified Electrodes. *Anal. Chem.* **2013**, *85*, 8158−8165.
(31) Cui, L.; Lu, M.; Li, Y.; Tang, B.; Zhang, C.-y. A Reusable Ratiometric Electrochemical Biosensor on the Basis of the Binding of Methylene Blue to DNA with Alternating AT Base Sequence for Sensitive Detection of Adenosine. *Biosens. Bioelectron.* **2018**, *102*, 87−93.
(32) Wang, Y.; Feng, J.; Tan, Z.; Wang, H. Electrochemical Impedance Spectroscopy Aptasensor for Ultrasensitive Detection of Adenosine with Dual Backfillers. *Biosens. Bioelectron.* **2014**, *60*, 218−223.
(33) Sun, A.; Wambach, T.; Venkatesh, A. G.; Hall, D. A. A Low-Cost Smartphone-Based Electrochemical Biosensor for Point-of-Care Diagnostics. *2014 IEEE Biomedical Circuits and Systems Conference (BioCAS)*, Lausanne, Switzerland; IEEE, 2014; pp 312−315.
(34) Aydoğdu Tığ, G. Highly Sensitive Amperometric Biosensor for Determination of NADH and Ethanol Based on Au-Ag Nanoparticles/Poly(L-Cysteine)/Reduced Graphene Oxide Nanocomposite. *Talanta* **2017**, *175*, 382−389.
(35) Mandal, R.; Baranwal, A.; Srivastava, A.; Chandra, P. Evolving Trends in Bio/Chemical Sensor Fabrication Incorporating Bimetallic Nanoparticles. *Biosens. Bioelectron.* **2018**, *117*, 546−561.
(36) Zeng, Y.; Zhu, Z.; Du, D.; Lin, Y. Nanomaterial-Based Electrochemical Biosensors for Food Safety. *J. Electroanal. Chem.* **2016**, *781*, 147−154.
(37) Aydemir, N.; Malmstrom, J.; Travas-Sejdic, J. Conducting Polymer Based Electrochemical Biosensors. *Phys. Chem. Chem. Phys.* **2016**, *18*, 8264−8277.
(38) Aydemir, N.; Chan, E.; Baek, P.; Barker, D.; Williams, D. E.; Travas-Sejdic, J. New Immobilisation Method for Oligonucleotides on Electrodes Enables Highly-Sensitive, Electrochemical Label-Free Gene Sensing. *Biosens. Bioelectron.* **2017**, *97*, 128−135.
(39) Guo, X.; Facchetti, A. The Journey of Conducting Polymers from Discovery to Application. *Nat. Mater.* **2020**, *19*, 922−928.
(40) Chen, J.; Xue, F.; Yu, Z.; Huang, L.; Tang, D. A Polypyrrole-Polydimethylsiloxane Sponge-Based Compressible Capacitance Sensor with Molecular Recognition for Point-of-Care Immunoassay. *Analyst* **2020**, *145*, 7186−7190.
(41) Cai, G.; Yu, Z.; Tang, D. Actuating Photoelectrochemical Sensing Sensitivity Coupling Core-Core-Shell Fe3O4@C@TiO2 with Molecularly Imprinted Polypyrrole. *Talanta* **2020**, *219*, 121341.

https://doi.org/10.1021/acsapm.1c01348
ACS Appl. Polym. Mater. 2021, 3, 6674−6683

(42) Yu, Z.; Cai, G.; Liu, X.; Tang, D. Platinum Nanozyme-Triggered Pressure-Based Immunoassay Using a Three-Dimensional Polypyrrole Foam-Based Flexible Pressure Sensor. *ACS Appl. Mater. Interfaces* **2020**, *12*, 40133−40140.
(43) Hira, S. A.; Yusuf, M.; Annas, D.; Nagappan, S.; Song, S.; Park, S.; Park, K. H. Recent Advances on Conducting Polymer-Supported Nanocomposites for Nonenzymatic Electrochemical Sensing. *Ind. Eng. Chem. Res.* **2021**, *60*, 13425−13437.
(44) Hira, S. A.; Nallal, M.; Rajendran, K.; Song, S.; Park, S.; Lee, J. M.; Joo, S. H.; Park, K. H. Ultrasensitive Detection of Hydrogen Peroxide and Dopamine Using Copolymer-Grafted Metal-Organic Framework Based Electrochemical Sensor. *Anal. Chim. Acta* **2020**, *1118*, 26−35.
(45) Zhang, Y.; Liu, S.; Wang, L.; Luo, Y.; Tian, J.; Asiri, A. M.; Al-Youbi, A. O.; Sun, X. Novel Use of Poly(3,4-Ethylenedioxythiophene) Nanoparticles for Fluorescent Nucleic Acid Detection. *ACS Comb. Sci.* **2012**, *14*, 191−196.
(46) Lu, L.; Zhang, O.; Xu, J.; Wen, Y.; Duan, X.; Yu, H.; Wu, L.; Nie, T. A Facile One-Step Redox Route for the Synthesis of Graphene/Poly (3,4-Ethylenedioxythiophene) Nanocomposite and Their Applications in Biosensing. *Sens. Actuators, B* **2013**, *181*, 567−574.
(47) Kaur, N.; Thakur, H.; Kumar, R.; Prabhakar, N. An Electrochemical Sensor Modified with Poly(3,4-Ethylenedioxythiophene)-Wrapped Multi-Walled Carbon Nanotubes for Enzyme Inhibition-Based Determination of Organophosphates. *Microchim. Acta* **2016**, *183*, 2307−2315.
(48) Thakur, H.; Kaur, N.; Sareen, D.; Prabhakar, N. Electrochemical Determination of M. Tuberculosis Antigen Based on Poly(3,4-Ethylenedioxythiophene) and Functionalized Carbon Nanotubes Hybrid Platform. *Talanta* **2017**, *171*, 115−123.
(49) Zeng, R.; Wang, W.; Chen, M.; Wan, Q.; Wang, C.; Knopp, D.; Tang, D. CRISPR-Cas12a-Driven MXene-PEDOT:PSS Piezoresistive Wireless Biosensor. *Nano Energy* **2021**, *82*, 105711.
(50) Zhang, R.; Jamal, R.; Ge, Y.; Zhang, W.; Yu, Z.; Yan, Y.; Liu, Y.; Abdiryim, T. Functionalized PProDOT@nitrogen-Doped Carbon Hollow Spheres Composites for Electrochemical Sensing of Tryptophan. *Carbon* **2020**, *161*, 842−855.
(51) Wei, B.; Ouyang, L.; Liu, J.; Martin, D. C. Post-Polymerization Functionalization of Poly(3,4-Propylenedioxythiophene) (PProDOT) via Thiol-Ene "Click" Chemistry. *J. Mater. Chem. B* **2015**, *3* (25), 5028−5034.
(52) Bhatt, M. P.; Thelen, J. L.; Balsara, N. P. Effect of Copolymer Composition on Electronic Conductivity of Electrochemically Oxidized Poly(3-Hexylthiophene)- b -Poly(Ethylene Oxide) Block Copolymers. *Chem. Mater.* **2015**, *27* (14), 5141−5148.
(53) Beaujuge, P. M.; Amb, C. M.; Reynolds, J. R. A Side-Chain Defunctionalization Approach Yields a Polymer Electrochrome Spray-Processable from Water. *Adv. Mater.* **2010**, *22* (47), 5383−5387.
(54) Mantione, D.; Casado, N.; Sanchez-Sanchez, A.; Sardon, H.; Mecerreyes, D. Easy-to-Make Carboxylic Acid Dioxythiophene Monomer (ProDOT-COOH) and Functional Conductive Polymers. *J. Polym. Sci., Part A: Polym. Chem.* **2017**, *55* (17), 2721−2724.
(55) Non-Aqueous Reference Electrode. *Ref. Mater.* **1995**; www.Basinc.com.
(56) *TECH TIP # 5: Attach an Antibody onto Glass, Silica or Quartz Surface*; Thermo Fisher Scientific Inc., 2015; www.thermo.com/pierce.
(57) Lane, R. F.; Hubbard, A. T. Electrochemistry of Chemisorbed Molecules. I. Reactants Connected to Electrodes through Olefinic Substituents. *J. Phys. Chem.* **1973**, *77*, 1401−1410.
(58) Abruña, H. D. Coordination Chemistry in Two Dimensions: Chemically Modified Electrodes. *Coord. Chem. Rev.* **1988**, *86*, 135−189.
(59) *EDC/NHS Crosslinking of Carboxylates with Primary Amines*; Thermo Fisher Scientific Inc., 2011; Vol. *0747*.
(60) Kim, C. O.; Hong, S. Y.; Kim, M.; Park, S. M.; Park, J. W. Modification of Indium-Tin Oxide (ITO) Glass with Aziridine Provides a Surface of High Amine Density. *J. Colloid Interface Sci.* **2004**, *277*, 499−504.
(61) Peng, H.; Soeller, C.; Vigar, N.; Kilmartin, P. A.; Cannell, M. B.; Bowmaker, G. A.; Cooney, R. P.; Travas-Sejdic, J. Label-Free Electrochemical DNA Sensor Based on Functionalised Conducting Copolymer. *Biosens. Bioelectron.* **2005**, *20*, 1821−1828.
(62) Xu, G.; Jarjes, Z. A.; Desprez, V.; Kilmartin, P. A.; Travas-Sejdic, J. Sensitive, Selective, Disposable Electrochemical Dopamine Sensor Based on PEDOT-Modified Laser Scribed Graphene. *Biosens. Bioelectron.* **2018**, *107*, 184−191.
(63) Loock, H. P.; Wentzell, P. D. Detection Limits of Chemical Sensors: Applications and Misapplications. *Sens. Actuators, B* **2012**, *173*, 157−163.
(64) Conigrave, A. D.; Van der Weyden, L.; Holt, L.; Jiang, L.; Wilson, P.; Christopherson, R. I.; Morris, M. B. Extracellular ATP-Dependent Suppression of Proliferation and Induction of Differentiation of Human HL-60 Leukemia Cells by Distinct Mechanisms. *Biochem. Pharmacol.* **2000**, *60*, 1585−1591.

https://doi.org/10.1021/acsapm.1c01348
ACS Appl. Polym. Mater. 2021, 3, 6674−6683